Yuzuncu Yil University
Journal of the Institute of Natural & Applied Sciences
https://dergipark.org.tr/en/pub/yyufbed

Research Article

ZnO/ITO, Sn and Cu Doped ZnO/ITO Films as an Photoanode for Solar Cell: Production and Characterizations †

İlker KARA*[1], Dheyaaldain Mohammed Hussein ALHASANI[1], Ahmet Furkan KAYIŞ[2], Özcan YALÇINKAYA [2], Olcay GENÇYILMAZ[1], Abjar Ibrahim Rashid HAFEDH[1]

[1]Çankırı Karatekin University, Graduate School of Natural and Applied Sciences, 18100, Çankırı, Türkiye
[2] Gazi University, Science and Art Faculty, Department of Chemistry, 06500, Ankara, Türkiye
İlker KARA, ORCID No: 0000-0003-3700-4825, Dheyaaldain Mohammed Hussein ALHASANI, ORCID No: 0009-0003-1635-0435, Ahmet Furkan KAYIŞ, ORCID No: 0000-0002-5412-2906, Özcan YALÇINKAYA, ORCID No: 0000-0002-2891-3878, Olcay GENÇYILMAZ, ORCID No: 0000-0002-7410-2937, Abjar Ibrahim Rashid HAFEDH, ORCID No: 0000-0001-5514-0404
*Corresponding author e-mail: ilkerkara@karatekin.edu.tr

Article Info

Received: 28.11.2023
Accepted: 24.04.2024
Online August 2024

DOI:10.53433/yyufbed.1397221

Keywords
Cu and Sn doping,
ITO,
SILAR method,
ZnO films

Abstract: Undoped ZnO and Sn- and Cu-doped ZnO thin films were fabricated on ITO substrates via the SILAR method for this study. The films were then subjected to structural, surface, optical, and electrical characterization. The undoped ZnO thin films displayed a spherical surface morphology, while the Sn-doped ZnO thin films exhibited a nano-flower surface morphology. On the other hand, the Cu-doped ZnO thin films demonstrated a relatively thicker and flat layer, as well as a fractured surface morphology that resulted in voids. The level of crystallization and transmittance values augmented upon doping. With Cu doping, n-p heterojunction structure was obtained from ZnO/ITO films. Hence, it is inferred that the generated Cu doped ZnO/ITO films can serve as alternative transparent conductive films (TCO) due to their low resistivity.

Güneş Pili için Fotoanot Olarak ZnO/ITO, Sn ve Cu Katkılı ZnO/ITO Filmleri: Üretim ve Karakterizasyonu

Makale Bilgileri

Geliş: 28.11.2023
Kabul: 24.04.202024
Online Ağustos 2024

DOI:10.53433/yyufbed.1397221

Anahtar Kelimeler
Cu ve Sn katkısı,
ITO,
SILAR yöntemi,
ZnO filmler

Öz: Bu çalışma için katkısız ZnO ve Sn- ve Cu katkılı ZnO ince filmler ITO alttaşlar üzerinde SILAR yöntemi ile üretilmiştir. Filmler daha sonra yapısal, yüzeysel, optik ve elektriksel karakterizasyona tabi tutulmuştur. Katkısız ZnO ince filmler küresel bir yüzey morfolojisi sergilerken, Sn katkılı ZnO ince filmler nano-çiçek yüzey morfolojisi sergilemiştir. Öte yandan, Cu katkılı ZnO ince filmler nispeten daha kalın ve düz bir tabakanın yanı sıra boşluklarla sonuçlanan kırık bir yüzey morfolojisi göstermiştir. Kristalleşme seviyesi ve geçirgenlik değerleri katkılamayla birlikte artmıştır. Cu katkısı ile ZnO/ITO filmlerinden n-p heteroeklem yapısı elde edildi. Bu nedenle, üretilen Cu katkılı ZnO/ITO ince filmlerin düşük dirençleri nedeniyle alternatif şeffaf iletken filmler (TCO) olarak hizmet edebileceği sonucuna varılmıştır.

† This study is produced from Master thesis "The Growth of Doped ZnO Thin Films by The SILAR Method and Investigation of Structural, Optical and Electrical Properties" prepared by Dheyaaldain Mohammed Hussein ALHASANI in 2023 under the supervision of Assoc. Prof. Dr. İlker KARA.

1. Introduction

Zinc oxide (ZnO) thin films are important II-VI semiconductors due to their significant exciton binding energy (60 meV) and wide band gap (approximately 3.3 eV) (Alwadai et al., 2021). The crystal structure of ZnO thin films is typically wurtzite (Devi et al., 2020). They have wide applications in various fields such as solar cells, gas sensors, light-emitting diodes (LEDs), laser systems, and transparent conductors due to their good structural, optical, and electrical qualities (Kaphle & Hari, 2018; Wang et al., 2018; Saini et al., 2020; Zhang et al., 2022; Saravanan et al., 2023; Rashid et al., 2024; Xiao et al., 2024). ZnO films have been extensively studied in recent years, particularly in the fields of optoelectronic devices and solar cells (Gençyılmaz, 2018; Klochko et al., 2018). They can be produced using various physical and chemical techniques. These techniques include magnetron sputtering, thermal evaporation, chemical bath deposition and pulsed laser deposition (PLD) (Li et al., 2024; Gençyılmaz et al., 2024; Alsultany et al., 2016; Thobega et al., 2024; Wang, 2023). Various techniques have been used for the synthesis of the material, including chemical vapour deposition, spray pyrolysis, sol-gel, and successive ionic layer adsorption technique (Devi et al., 2020; Li et al., 2024; Kumar et al., 2018; Saravanan et al., 2023; Cruz et al., 2023; Şahin et al., 2022; Ashith et al., 2018). Among these techniques, the SILAR technique stands out due to its practicality, economy, and reproducibility.

However, the physical properties of ZnO films vary depending on the size, orientation, and surface quality of the grains, as well as the conditions under which the material is prepared and the processes used. The technique employed in production, the substrate on which the films are deposited, and the doping process significantly affects the physical properties of the films. In particular, the structural characteristics of ZnO films are greatly influenced by the substrate used in their formation. Various studies in the literature have investigated the use of substrates such as silicon, quartz, sapphire, FTO, and ITO in the production of ZnO (Tang et al., 2024; Solaymani et al., 2021; Chaitra et al., 2021; Klochko et al., 2019). Recently, metal doping of ZnO films with Ga, Ti, Al, Si, Sn, and Cu has led to the development of materials with enhanced optical characteristics and high conductivity (Dhamodharan et al., 2015).

The study employed the SILAR process to produce ZnO films on ITO substrates. The films were either undoped or doped with Sn and Cu. The impact of Sn and Cu doping on the electrical, surface, structural, and optical characteristics of ZnO films grown on an ITO substrate was investigated.

2. Material and Methods

The Successive Ionic Layer Adsorption and Reaction (SILAR) method is an economical and flexible technique for creating thin films (Kadem et al., 2017). It has a wide range of applications in scientific research, materials science, solar cells, sensors, and optoelectronic devices. The SILAR method enables precise control over the thickness and desired properties of thin films, making it a straightforward and accessible means of regulating their growth. The study involved the growth of undoped, Sn-doped and Cu-doped ZnO films using the SILAR method.

2.1. Preparation of substrate materials

ZnO, Sn and Cu doped ZnO films were grown on an indium tin oxide (ITO) substrate. The ITO coated glass materials used were TEC8 model, 25 mm x 25 mm, 2 mm thick. Prior to modification, the ITO coated glasses underwent cleaning. They were first rinsed in soapy water to remove any material, and then cleaned using an ultrasonic cleaner and acetone for ten minutes. Finally, they were washed using an ultrasonic cleaner for 10 minutes in a 1:1 ethanol-water solution.

2.2. Production process

($[Zn(NH_3)_4]^{2+}$) zinc-ammonia complex was used to grow ZnO thin films on ITO substrate. To prepare the zinc-ammonia solution complex, 0.1 M $ZnCl_2$ (pH≈5.5) and 25 - 28 % NH_3 solutions were mixed in 1 to 10 molar ratio [$Zn:NH_3$=1:10] (Figure 1). The following Equations 1, 2, 3, and 4 explain the chemical reactions that occur during the growth phase of thin films (Rajamanickam et al., 2024);

$$ZnCl_2 + 2NH_4OH \leftrightarrow Zn(OH)_2 + 2NH_4^+ + 2Cl^- \quad (1)$$

$$Zn(OH)_2 + 4NH_4^+ \leftrightarrow [Zn(NH_3)_4]^{2+} + 2H_2O + 2H^+ \quad (2)$$

$$[Zn(NH_3)_4]^{2+} + 4H_2O \rightarrow Zn(OH)_2\,(s) + 4NH_4^+ + 2OH^- \quad (3)$$

$$Zn(OH)_2\,(s) \rightarrow ZnO(s) + H_2O \quad (4)$$

In order to generate films of Sn-doped ZnO and Cu-doped ZnO, the ITO substrate had to be cleaned. Following the cleaning process, solutions were mixed according to the specified additive ratio. Then, using the SILAR approach, thin films of zinc oxide (ZnO) doped with Sn and Cu were grown on an indium tin oxide (ITO) substrate.

When the $ZnCl_2$, $SnCl_2$, $CuCl_2$, and NH_3 solutions are mixed together, a complex of $[Zn(NH_3)_4]^{2+}$, ($[Sn(NH_3)_4]^{2+}$, and $(Cu(NH_3)_4]^{2+}$ (pH10) is formed. Keeping the Sn concentration fixed at 1% and Cu concentration at 1%, thin films of Sn-doped and Cu-doped ZnO were grown on ITO (Indium Tin Oxide) substrates by mixing $[Zn(NH_3)_4]^{2+}$ and $[Cu(NH_3)_4]^{3+}$ complexes and following the aforementioned growth stages. Figure 1 and Figure 2 shows a schematic representation of the SILAR technique used in ZnO films on ITO substrate and Schematic representation of the application of the two-point probe technique to films, respectively.

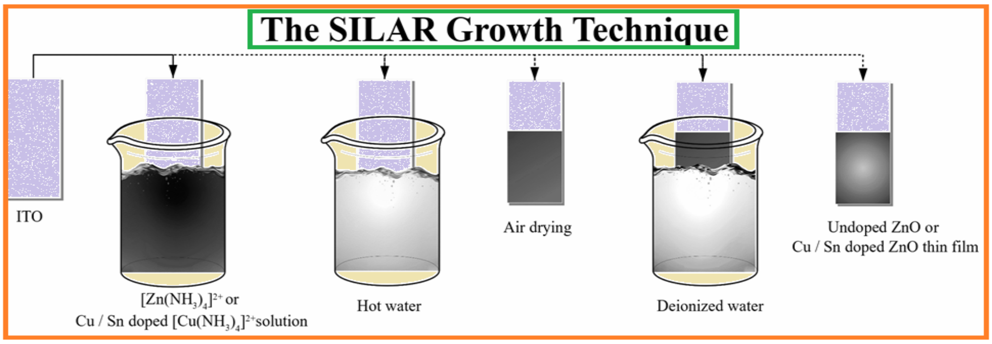

Figure 1. ZnO films on ITO substrate using SILAR method growth process.

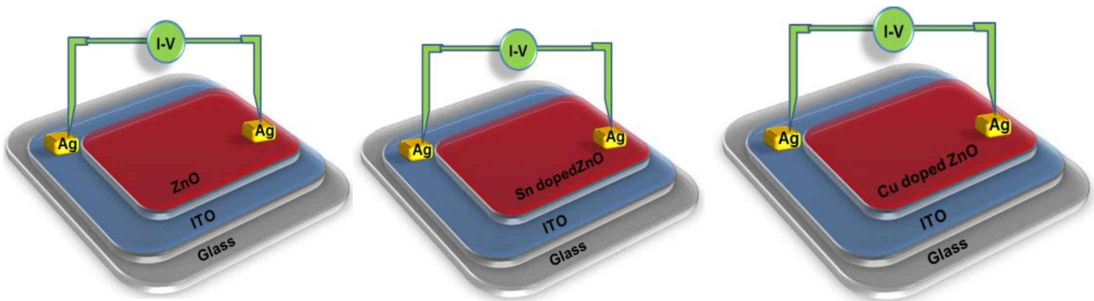

Figure 2. Schematic representation of the application of the two-point probe technique to films.

Research was conducted on films of ZnO, Sn, and Cu-doped ZnO that were formed on an ITO substrate to determine their electrical, structural, surface, and optical characteristics. Various imaging techniques, including X-ray diffractometers, field emission scanning electron microscopy, a UV-VIS spectrophotometer, and a current-voltage measuring device, were used to characterize the necessary attributes. Absorbance and transmittance spectra were obtained from UV-vis spectrometer analyses. The films were analyzed using an APD 2000 PRO XRD device to calculate their spectra, band structure, and band gap energies. The X-ray results were used to determine the films' crystallization levels, half-peak widths, and Miller indices. Additionally, the films' electrical characteristics were examined using the two-point probe technique. Voltages ranging from -3 to +3 volts were applied by making contact at two different points on the films. The resulting current values were used to draw I-V graphs and determine the transmission mechanisms. Additionally, electrical characteristics such as ideality factor and barrier height were computed for the ZnO sheets. Field emission scanning electron microscopy (FESEM) was used to examine the films' morphological qualities and determine the effect of the base on their surface properties. Surface images of the films were obtained and analyzed to understand the substrate's impact on the surface attributes.

3. Results

X-ray diffraction was used to determine the mode of crystal growth and the phases in which the produced material was formed. The X-ray diffraction patterns revealed a polycrystalline hexagonal (wurtzite) structure of the ZnO thin films produced on a glass substrate at room temperature (Figure 3). These results are consistent with previous findings on ZnO produced using the SILAR method (Alsuntany et al., 2016; Kadem et al., 2017). Figure 3 shows the XRD analysis results of undoped ZnO, Sn-doped ZnO, and Cu-doped ZnO thin films. As shown in Figure 3(a), the dominant diffraction peaks correspond to the ITO substrate, exhibiting the (101), (111), and (002) orientations characteristic of the tetragonal crystal structure. The Cu-doped ZnO films exhibit the most prominent diffraction peaks at (101), (111), and (002), while the Sn-doped ZnO films exhibit the most prominent peaks at (101), (111), and (002). The crystallization levels of the films indicate that the Cu-doped ZnO film is the most compatible, while the undoped ZnO thin film has an amorphous-like structure.

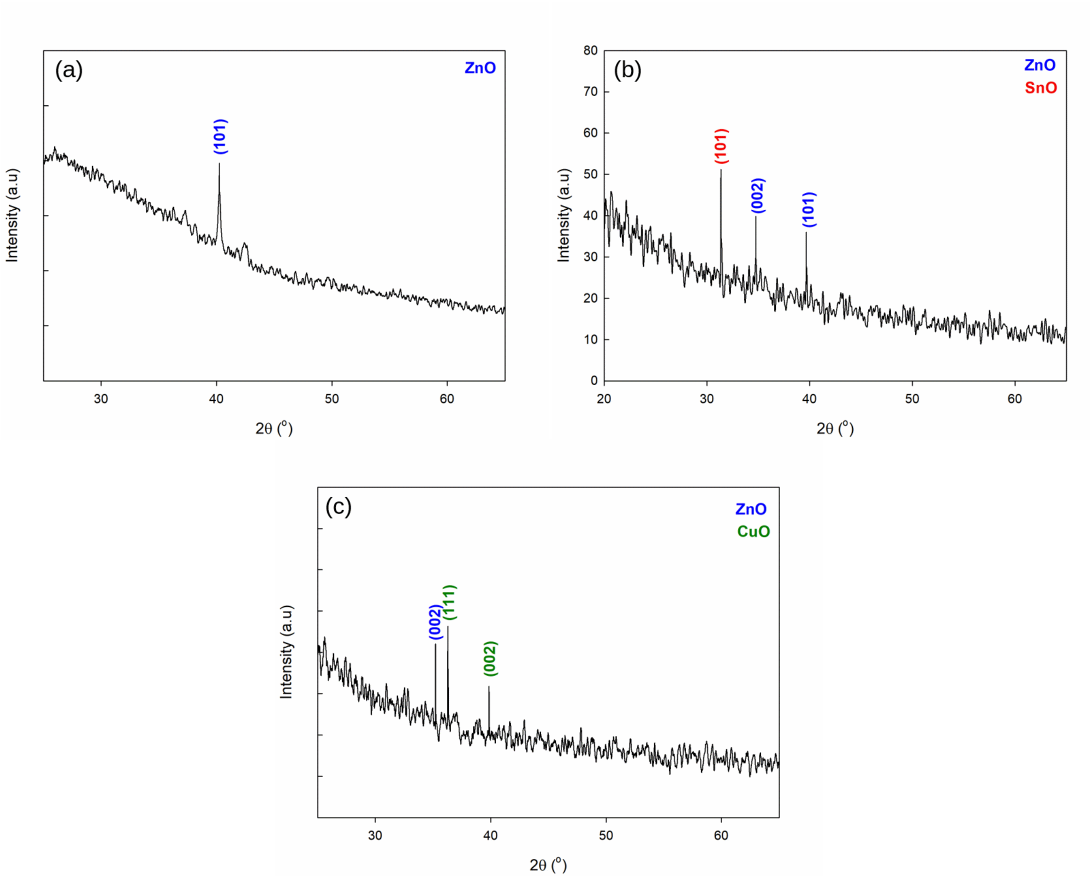

Figure 3. XRD analysis of ITO/ZnO, Sn-doped ZnO, Cu-doped ZnO thin films.

Figure 4 presents FESEM/EDS images of ZnO, Sn and Cu doped ZnO films. The undoped ZnO films exhibit spherical formations on their surface, which appear as a thin layer on the ITO substrate with voids in some regions. In contrast, the Sn-doped ZnO thin films exhibit the growth of nanoflower structures on the ITO substrate, which coalesce in certain regions to form broken layers, while voids are present in other regions. Cu-doped ZnO films form an even layer on the ITO substrate, which is affected by the surface shape. However, this layer may exhibit fractures that create voids in certain areas. These fractures are caused by surface tension during the film growth process.

EDS measurements were performed to understand the elemental composition and compositional ratios of the grown undoped ZnO, Sn-doped ZnO and Cu-doped ZnO samples. The relevant images are given in Figure 4. The EDS spectra of the samples indicate the presence of Al, Si, O, C, and Mg. The presence of Si in the EDS spectrum is attributed to the precursor materials used in the synthesis process and the glass substrate. The presence of magnesium indicates an undesirable impurity during the film synthesis stage. For SEM/EDS analysis of the samples, aluminum studs were used, which explains the presence of the element Al in the studied EDS spectra.

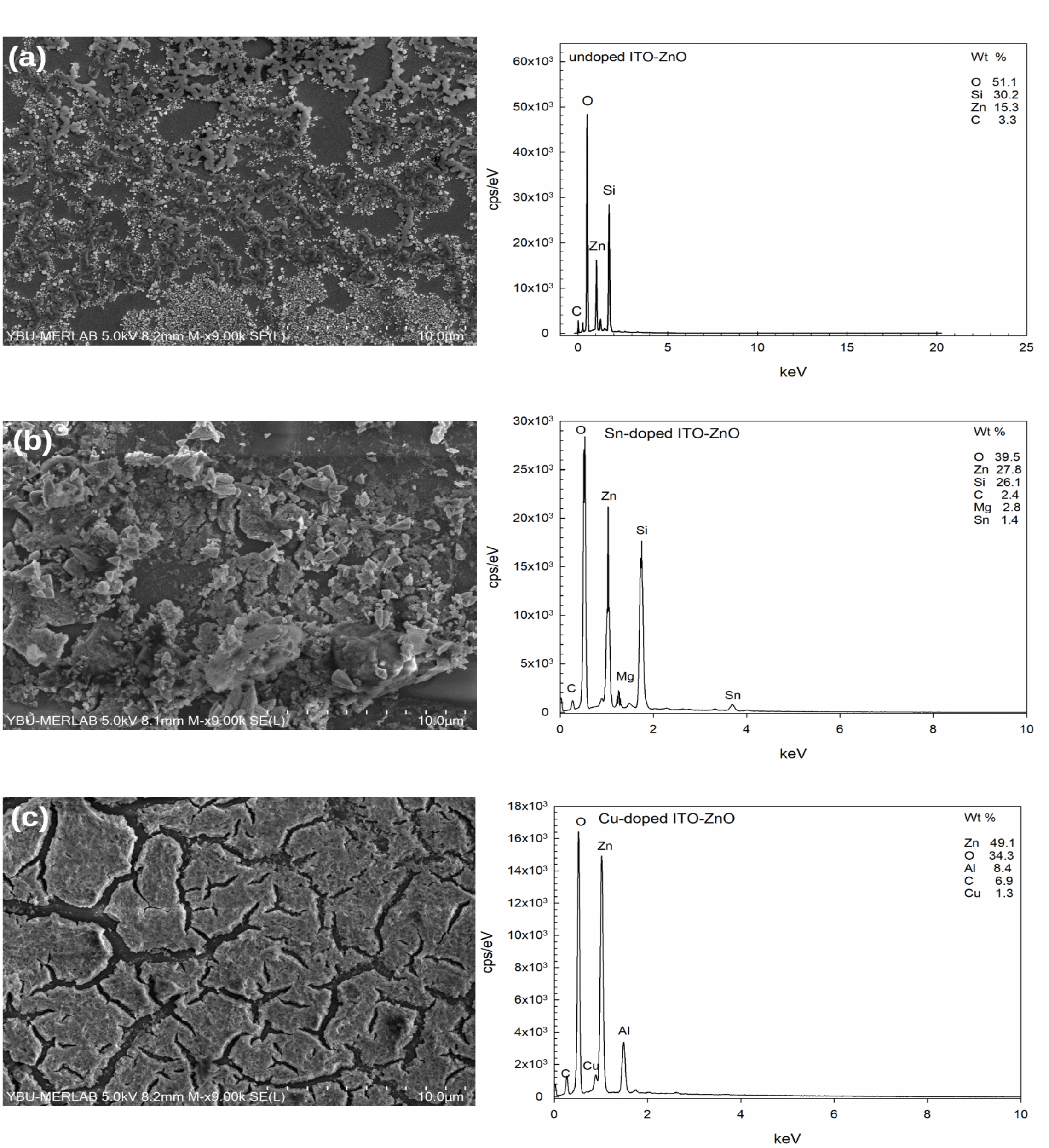

Figure 4. FESEM and EDS analyzes of ITO/ZnO, Sn doped ITO/ZnO, Cu doped ZnO thin films.

The absorbance and transmittance spectra, obtained by measuring the absorption at room temperature, of the undoped ZnO, Sn-doped ZnO, and Cu-doped ZnO thin film samples grown using the SILAR technique, are presented in Figure 5. Sharp and clear band edge formation was observed in all films at wavelengths of less than 300 nm. Figure 5 (b) indicates that the permeability values of ZnO films grown on ITO substrate with Sn and Cu doping increased. Furthermore, the absorption band edges of the films became smoother with the doping of Sn and Cu.

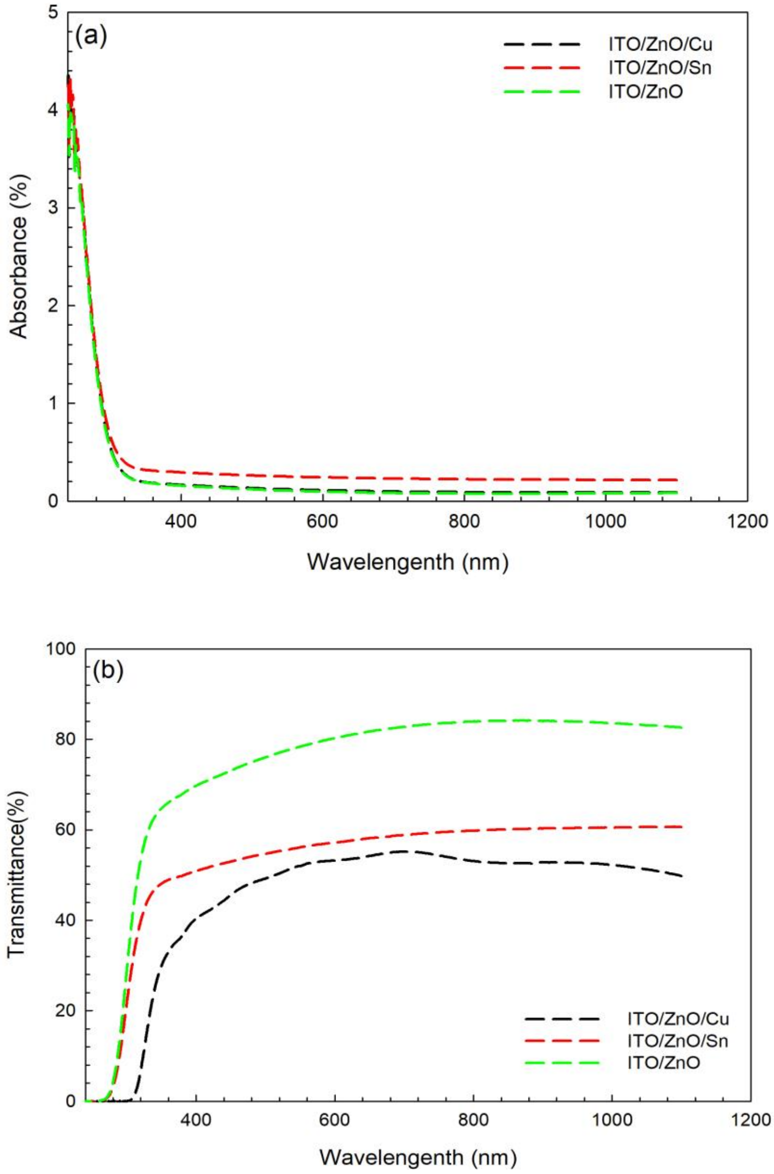

Figure 5. Absorbance and transmittance spectra of (a) ZnO/ITO, (b) Sn doped ZnO/ITO, (c) Cu doped ZnO/ITO films.

Using absorption measurements, the graph of $(\alpha h\nu)^2$ $(eV.cm^{-1})^2$ as a function of energy was also plotted and the band gap energy (E_g) of the films was calculated, as shown in Figure 6. The bandgap energy values were observed to increase for Sn-doped ZnO thin films, while they decreased for Cu-doped ZnO thin films. These values are consistent with the literature (Kadem et al., 2017).

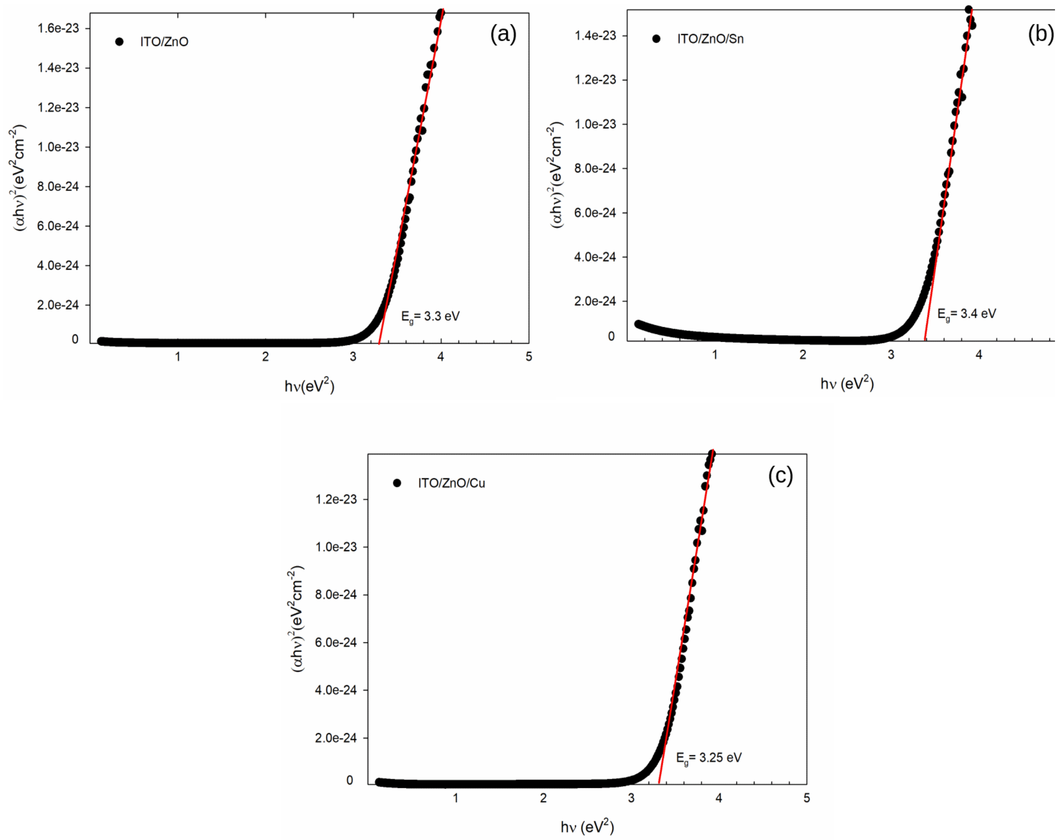

Figure 6. $(\alpha h\nu)^2$ $(\text{eVcm}^{-1})^2$ plots of (a) ZnO/ITO, (b) Sn doped ZnO/ITO, (c) Cu doped ZnO/ITO films.

The current-voltage variation was recorded for all samples at room temperature and light between -3V and +3V, as shown in Figure 7 after contact with Ag. ZnO films exhibit behavior that is more similar to that of metals when studying the properties (Current - Voltage) in the dark and the effect of doping on the electrical resistance of ZnO films. All the ZnO thin film exhibits n-type conductivity in this study. However, it does sometimes show semi-conductive properties because it behaves in a manner that is between metals and semiconductors. The log I-V plots of heterostructure are shown in Figure 7. The electrical parameters are given in Table 1. The following relations were used (Sze, 1981);

$$I = I_0\left[\left(e^{\frac{qV}{nkT}}\right) - 1\right] \qquad (5)$$

where I_0 is reverse saturation current, q is electronic charge, V is applied voltage, k is Boltzman constant, n is ideality factor and T is temperature (in Kelvin).

$$I_0 = AA^*T^2 e^{\left(\frac{-q\phi_B}{kT}\right)} \qquad (6)$$

where A is contact area, A^* is Richardson constant and ϕ_B is barrier height at zero bias. The slope obtained from the I-V graph was used to find the n value and it was found with the Equation 7 obtained from the Equation 6.

$$\text{n}=\frac{\text{q}}{\text{kT}}\left(\frac{\text{dV}}{\text{d(ln (I)}}\right) \qquad (7)$$

barrier height was calculated with Equation (8).

$$\phi_B = \frac{kT}{kq} \ln\left(\frac{AA^{*}T^{2}}{Io}\right) \quad (8)$$

Table 1 gives these calculated electrical parameters. The lowest ideality factor was observed in the Cu-doped ZnO thin film, while the highest was seen in the undoped ITO/ZnO thin film. The higher ideality factor value of Sn-doped ZnO films compared to Cu-doped ZnO films can be expalined to the presence of natural oxide on the ITO layer and/or high oxygen deficiency (Asghar et al., 2013). Besides, it can be attributed to the improvement in surface morphology and reduction in roughness values with the increase in thickness of the Cu-doped ZnO thin film on the substrate surface. The ZnO/ITO and Sn-doped ZnO/ITO films exhibited an ohmic conduction mechanism and lower resistance than the Cu-doped ZnO/ITO films. The Cu-doped ZnO/ITO films deviated from ohmic behaviour, exhibiting lower resistance with Cu doping and diode properties. The high resistivity of the ZnO-rich thin film is attributed to both grain boundary effects and the semiconducting nature of ZnO. The semiconducting nature of ZnO creates a potential barrier that affects electrical transport, resulting in decreased conductivity. In addition, the increase in the conductivity of Cu-doped ZnO/ITO films may be due to the reduction of oxidations in the structure. The logarithmic current–voltage characteristics of the undoped ZnO/ITO, Sn doped ZnO/ITO and Cu doped ZnO/ITO films are shown in Figure 8. At room temperature for Cu-doped ZnO films is non-linear, indicating the formation of an p-n junction in Cu-doped ZnO/ITO films. In terms of electrical properties, Cu-doped ZnO has been shown to be the superior layer.

Table 1. The electrical parameters of ZnO/ITO, Sn doped ZnO/ITO and Cu doped ZnO/ITO films

Films	**I_0 (A)**	**n**	**ϕ_B (eV)**
Undoped ZnO/ITO	1.43×10^{-7}	4.07	0.789
Sn doped ZnO/ITO	1.01×10^{-5}	4.05	0.761
Cu doped ZnO/ITO	7.13×10^{-8}	3.65	0.695

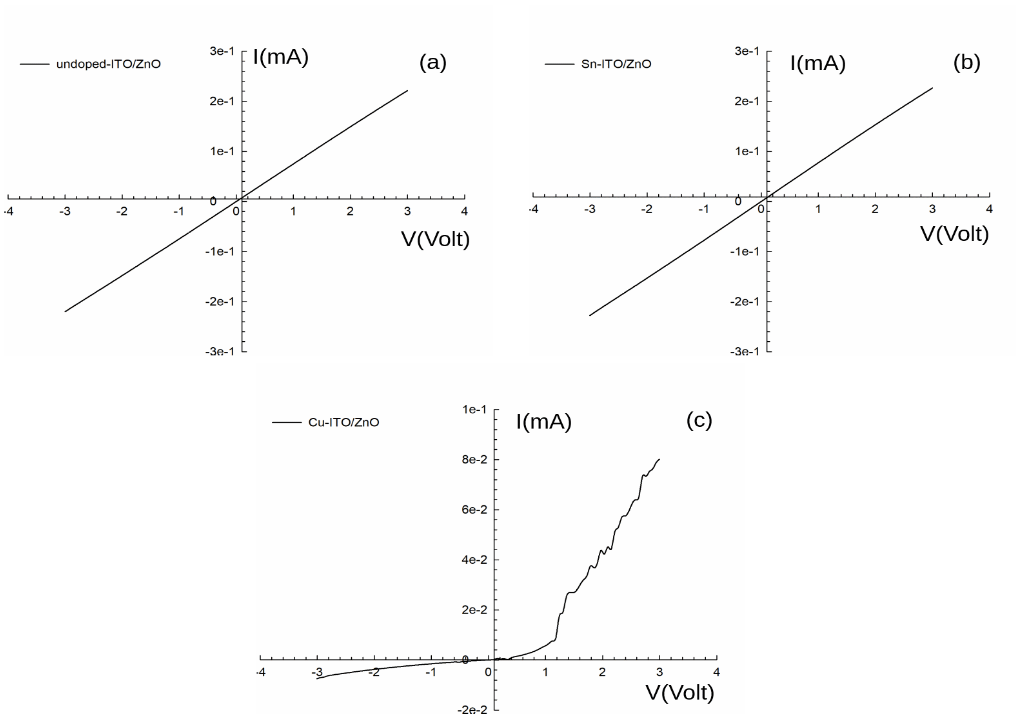

Figure 7. I-V plots of (a) ZnO/ITO, (b) Sn doped ZnO/ITO, (c) Cu doped ZnO/ITO films.

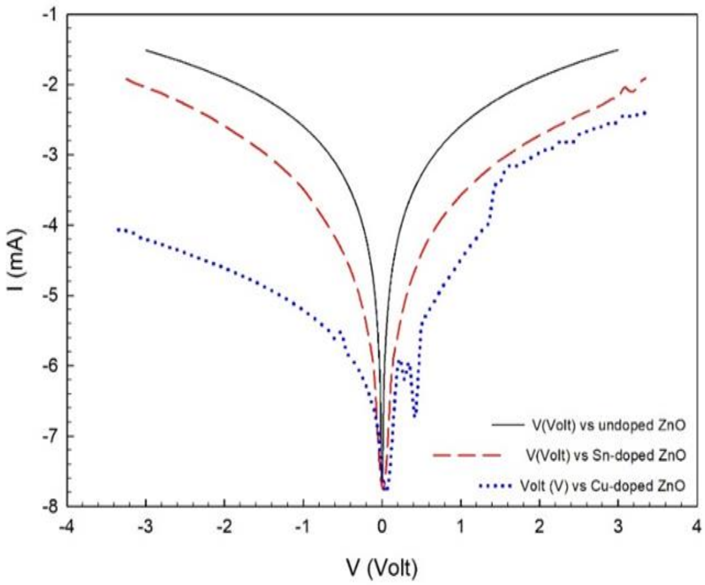

Figure 8. The log I-V plots of (a) ZnO/ITO, (b) Sn doped ZnO/ITO, (c) Cu doped ZnO/ITO films.

4. Discussion

The many desirable optical and electrical properties of ZnO films make it an attractive material for use in sensor development. Doping processes are widely used by researchers to improve the physical and electrical properties of metal oxide semiconductors. In recent years, the SILAR (Sequential Ionic Layer Adsorption and Reaction) method has gained significant popularity compared to other methods in the production of ZnO thin films. This is due to its advantages such as being cost-effective, safe, easy to apply and easy to control various parameters during the synthesis process.

In this study, ZnO, Sn-doped and Cu-doped thin films were successfully grown on ITO substrate using the SILAR technique. In the XRD data analysis results, when the crystallization levels of the films were examined, it was seen that all of the pure ZnO thin films exhibited crystal structure. However, it was determined that Cu doping was more effective in improving the crystal structure of ZnO films than Sn doping. This situation can be examined through studies at different contribution rates. EDS spectra of the produced samples revealed the presence of elements such as Al, Si, O, C and Mg. The presence of Si in the EDS spectra can be attributed to the glass substrate used as the base material in the synthesis process. The presence of Mg is probably due to an undesirable impurity in the film synthesis stage. More suitable production environments can be provided for the removal of such impurities. The band gap energy (Eg) values of the produced thin films are in agreement with the literature.

It was observed that the band gap energy values increased in Sn-doped ZnO thin films and decreased in Cu-doped ZnO thin films. When electrical analyzes were examined, it was determined that Cu doped ZnO/ITO films would be more suitable than other films for solar cells and gas sensor applications.

5. Conclusion

In this study, ZnO/ITO, Sn-doped ZnO/ITO and Cu-doped ZnO/ITO layered heterostructure films were successfully produced using the SILAR technique. All films exhibited wurtzite polycrystalline structure and high crystallization level. Cu doping increased the crystallization level more than Sn doping. While the surface morphology showed nanoflower-like structures with Sn doping, the surface morphology completely changed with Cu doping. With the addition of Cu, films with more homogeneous and fractured surface morphology were obtained. The permeability values of ZnO/ITO films were increased by 40% and 20% with the addition of Sn and Cu. While the ZnO/ITO band gap value was increased to 3.4 eV with Sn doping, films with a narrower band gap of 3.25 eV were obtained with Cu doping. P-n type conduction feature was imparted to ZnO/ITO films with Cu doping.

References

Alsultany, F. H., Hassan, Z., & Ahmed, N. M. (2016). Catalyst-free growth of ZnO nanowires on ITO seed layer/glass by thermal evaporation method: effects of ITO seed layer laser annealing temperature. *Superlattices and Microstructures*, *92*, 68-79. https://doi.org/10.1016/j.spmi.2016.01.038

Alwadai, N., Mitra, S., Hedhili, M. N., Alamoudi, H., Xin, B., Alaal, N., & Roqan, I. S. (2021). Enhanced-performance self-powered solar-blind UV-C photodetector based on n-ZnO quantum dots functionalized by p-CuO micro-pyramids. *ACS Applied Materials & Interfaces*, *13*(28), 33335-33344. https://doi.org/10.1021/acsami.1c03424

Asghar, M., Mahmood, K., Faisal, M., & Hasan, M. A. (2013). Electrical characterization of Au/ZnO/Si Schottky contact. *Journal of Physics: Conference Series*, *439*(1), 012030. https://doi.org/10.1088/1742-6596/439/1/012030

Ashith, V. K., Rao, G. K., Moger, S. N., & Smitha, R. (2018). Effect of post-deposition annealing on the properties of ZnO films obtained by high temperature, micro-controller based SILAR deposition. *Ceramics International*, *44*(9), 10669-10676. https://doi.org/10.1016/j.ceramint.2018.03.097

Chaitra, U., Ali, A. M., Mahesha, M. G., Kompa, A., Kekuda, D., & Rao, K. M. (2021). Property evaluation of spin coated Al doped ZnO thin films and Au/AZO/FTO Schottky diodes. *Superlattices and Microstructures*, *155*, 106903. https://doi.org/10.1016/j.spmi.2021.106903

Cruz, M. A., Saldaña-Ramírez, A., Juárez-Ramírez, I., & Torres-Martínez, L. M. (2023). Development of SnO2–ZnO thin films as a photocatalyst for obtaining alternative fuels through photocatalytic reactions. *Solid State Sciences*, *137*, 107112. https://doi.org/10.1016/j.solidstatesciences.2023.107112

Devi, K. R., Selvan, G., Karunakaran, M., Raj, I. L. P., Ganesh, V., & AlFaify, S. (2020). Enhanced room temperature ammonia gas sensing properties of strontium doped ZnO thin films by cost-effective SILAR method. *Materials Science in Semiconductor Processing*, *119*, 105117. https://doi.org/10.1016/j.mssp.2020.105117

Dhamodharan, P., Manoharan, C., Dhanapandian, S., Bououdina, M., & Ramalingam, S. (2015). Preparation and characterization of spray deposited Sn-doped ZnO thin films onto ITO subtracts as photoanode in dye sensitized solar cell. *Journal of Materials Science: Materials in Electronics*, *26*, 4830-4839. https://doi.org/10.1007/s10854-015-2990-7

Gençyılmaz, O. (2018). The effect of different cobalt precursors on the Co doped ZnO films produced by ultrasonic spray pyrolysis. *Journal of Nanoelectronics and Optoelectronics*, *13*(4), 509-520. https://doi.org/10.1166/jno.2018.2288. https://doi.org/10.1166/jno.2018.2288

Gençyılmaz, O., Akyüz, İ., & Atay, F. (2024). Binary ZnS–ZnO films as an alternative buffer layer for solar cell applications. *Applied Physics A*, *130*(4), 227. https://doi.org/10.1007/s00339-024-07382-1

Kadem, B., Banimuslem, H. A., & Hassan, A. (2017). Modification of morphological and optical properties of ZnO thin film. *Karbala International Journal of Modern Science*, *3*(2), 103-110. https://doi.org/10.1016/j.kijoms.2017.04.003

Kaphle, A., & Hari, P. (2018). Enhancement in power conversion efficiency of silicon solar cells with cobalt doped ZnO nanoparticle thin film layers. *Thin Solid Films*, *657*, 76-87. https://doi.org/10.1016/j.tsf.2018.05.014

Klochko, N. P., Kopach, V. R., Tyukhov, I. I., Zhadan, D. O., Klepikova, K. S., Khrypunov, G. S., ... & Khrypunova, A. L. (2018). Metal oxide heterojunction (NiO/ZnO) prepared by low temperature solution growth for UV-photodetector and semi-transparent solar cell. *Solar Energy*, *164*, 149-159. https://doi.org/10.1016/j.solener.2018.01.054

Klochko, N. P., Klepikova, K. S., Kopach, V. R., Tyukhov, I. I., Starikov, V. V., Sofronov, D. S., ... & Khrypunova, A. L. (2019). Development of semi-transparent ZnO/FTO solar thermoelectric nanogenerator for energy efficient glazing. *Solar Energy*, *184*, 230-239. https://doi.org/10.1016/j.solener.2019.04.002

Kumar, A., Joseph, S., Tsechansky, L., Privat, K., Schreiter, I. J., Schüth, C., & Graber, E. R. (2018). Biochar aging in contaminated soil promotes Zn immobilization due to changes in biochar surface structural and chemical properties. *Science of the Total Environment*, *626*, 953-961. https://doi.org/10.1016/j.scitotenv.2018.01.157

Li, L., Gao, S., Zhang, Z., Tang, Y., Zhao, Y., Guo, J., & Yang, P. (2024). Optical control of Cu/ZnO composite film for solar battery. *Chemical Physics Letters*, *839*, 141110. https://doi.org/10.1016/j.cplett.2024.141110

Rajamanickam, S., Mohammad, S. M., Razak, I. A., Abed, S. M., & Muhammad, A. (2024). Enhanced performance of PFO-ZnO nanorods nanocomposite photodiodes grown on ZnO NRs/ZnO/ITO-coated glass. *Optical Materials*, *148*, 114818. https://doi.org/10.1016/j.optmat.2023.114818

Rashid, M. H., Sujoy, S. I., Rahman, M. S., & Haque, M. J. (2024). Aloe vera assisted green synthesis of Ag and Cu co-doped ZnO nanoparticles and a comprehensive analysis of their structural, morphological, optical, electrical and antibacterial properties. *Heliyon*, *10*(3), e25438. https://doi.org/10.1016/j.heliyon.2024.e25438

Saini, M., Singh, R., Mitra, A., & Som, T. (2020). Photoresponse of pulsed laser deposited ZnO: Cu thin films. *Solar Energy*, *207*, 228-234. https://doi.org/10.1016/j.solener.2020.06.072

Saravanan, K., Sen, S., Sharma, C., Amirthapandian, S., Ganesan, K., Gupta, M., ... & Shekar, N. C. (2023). Room temperature excitonic emission in highly aligned ZnO nanostructures prepared by glancing angle Xe+ ion irradiation. *Journal of Luminescence*, *263*, 120059. https://doi.org/10.1016/j.jlumin.2023.120059

Solaymani, S., Ţălu, Ş., Nezafat, N. B., Dejam, L., Shafiekhani, A., Ghaderi, A., & Zelati, A. (2021). Optical properties and surface dynamics analyses of homojunction and heterojunction Q/ITO/ZnO/NZO and Q/ITO/ZnO/NiO thin films. *Results in Physics*, *29*, 104679. https://doi.org/10.1016/j.rinp.2021.104679

Sze, S. M. (1981). *Physics of semiconductor devices* (2nd ed.). Newyork, USA:Wiley.

Şahin, B., Aydin, R., Soylu, S., Türkmen, M., Kara, M., Akkaya, A., ... & Ayyıldız, E. (2022). The effect of thymus syriacus plant extract on the main physical and antibacterial activities of ZnO nanoparticles synthesized by SILAR method. *Inorganic Chemistry Communications*, *135*, 109088. https://doi.org/10.1016/j.inoche.2021.109088

Tang, Z., Fan, Z. Y., Fang, J. L., Zhang, L., Sun, Q. J., Zhang, D., ... & Jiang, X. (2024). Transparent artificial synapses based on Ag/Al-doped ZnO/ITO memristors for bioinspired neuromorphic computing. *Materials Letters*, *354*, 135342. https://doi.org/10.1016/j.matlet.2023.135342

Thobega, M., Maabong-Tau, K., Lefatshe, K., & Muiva, C. (2024). Study of structural, optical and electrical properties of Nickel doped ZnO (Ni–ZnO) nanorods grown by chemical bath deposition. *Physica B: Condensed Matter*, *673*, 415500. https://doi.org/10.1016/j.physb.2023.415500

Wang, C. F., Liu, N., & Hu, B. (2018). Improved white light emission from ZnS: Mn/ZnO/GaN core-shell nanorods array. *Journal of Luminescence*, *204*, 424-427. https://doi.org/10.1016/j.jlumin.2018.08.048

Wang, C. (2023). Fabrication and optical-electrical characteristics of ZnS/ZnO films by pulsed laser deposition. *Thin Solid Films*, *780*, 139971. https://doi.org/10.1016/j.tsf.2023.139971

Xiao, D., Wang, Y., Zhang, D., Liu, Y., Wang, H., Li, Y., ... & Sun, M. (2024). CuO/ZnO hollow nanocages derived from metal− organic frameworks for ultra-high and rapid response H2S gas sensor. *Ceramics International*, *50*, 15767-15779. https://doi.org/10.1016/j.ceramint.2024.02.057

Zhang, D., Liu, Y. H., & Zhu, L. (2022). Surface engineering of ZnO nanoparticles with diethylenetriamine for efficient red quantum-dot light-emitting diodes. *Iscience*, *25*, 105111. https://doi.org/10.1016/j.isci.2022.105111